Arch. Metall. Mater. **71** (2026), 2, 579-582

DOI: https://doi.org/10.24425/amm.2026.158845

JOOWON SUH[1†], SEUNGMUN JUNG[1†], WONJONG JEONG[2], HO JIN RYU[3], SUK HOON KANG[1*]

EFFECT OF CERAMIC CRUCIBLE (Al_2O_3 OR MgO) ON Y PRE-ALLOYED FERRITIC STEEL FABRICATED BY VACUUM INDUCTION MELTING

In this study, yttrium (Y) pre-alloyed ferritic steel was produced by vacuum induction melting casting. During casting, two types of ceramic crucible, Al_2O_3 and MgO, were used. The initial Y content was set to 1.2 wt.% in Fe-14.6Cr (in wt.%) ferritic steel. Inductively coupled plasma-atomic emission spectroscopy revealed that the remaining Y content was 0.04 wt.% in ferritic steel using an Al_2O_3 crucible, compared with 1.06 wt.% in steel using an MgO crucible. Energy dispersive X-ray spectroscopy analysis confirmed the formation of Y-Al-O oxides in ferritic steel (Al_2O_3), while X-ray diffraction detected the Fe_5Y phase in ferritic steel (MgO). According to reported Y_2O_3-Al_2O_3 and Y_2O_3-MgO phase diagrams, the Y_2O_3 is insoluble in Al_2O_3 but soluble to MgO. These results indicate that MgO crucible is more suitable for preventing Y loss during vacuum induction melting.

Keywords: Yttrium pre-alloyed; ferritic steel; vacuum induction melting; MgO crucible; preventing Y loss

1. Introduction

Yttrium (Y) is a Group 3 rare earth element and is crucial to enhance mechanical properties [1] in the form of Y_2O_3 nano oxide, as well as corrosion resistance [2] through the formation of Y_2O_3 protective layer. In particular, thermally stable Y_2O_3 nanoparticles effectively restrict dislocation movement and grain growth. Consequently, Y_2O_3-based oxide dispersion strengthened (ODS) steels are considered candidate structural materials for fission and fusion reactors [3,4].

To date, ODS steels have generally been fabricated using powder metallurgy process. In this approach, Y_2O_3 nanoparticles are dispersed into steel powder by ball milling, followed by hot consolidation and thermomechanical treatment [5]. However, the cost effectiveness of producing ODS steel powder via ball milling is challenging [6].

Recently, ODS steels have been fabricated using Y pre-alloyed gas atomized powders as an alternative to ball milling [7,8]. The Y pre-alloyed powder is oxidized to form a thin Fe-O or Cr-O oxide layer on the surface of powder, which subsequently evolves into Y_2O_3 during thermomechanical treatment. Prior to producing Y pre-alloyed steel powders, all pure elements are charged and melted in a ceramic crucible [9]. Therefore, studying the reaction between Y retained steel and ceramic crucibles is essential to prevent Y loss, as Y has a strong oxygen affinity.

This study aims to fabricate Y pre-alloyed steel and to investigate the reactions between Y retained steel and ceramic crucible. For this purpose, material was produced by vacuum induction melting (VIM) because VIM processed Y retained steel serves as feedstock for gas atomization, and the molten steel experiences direct interaction with the ceramic crucible during VIM. Fe-14.5Cr ferritic steel was selected as the base steel, as it has been widely studied for ODS steel applications. Al_2O_3 and MgO were chosen as ceramic crucibles for the VIM process. The effects of Y retained steel and crucible were systematically investigated. It was demonstrated that the crucible-dependent interfacial reactions during VIM were identified as the governing factor for Y retention in Y pre-alloyed steels, with MgO crucible suppressing Y loss, unlike Al_2O_3 crucible which promotes Y-Al-O oxide formation.

2. Experimental

Materials were produced by vacuum induction melting (VIM, MetalMate, Republic of Korea). Initially, high purity Fe,

[1] KOREA ATOMIC ENERGY RESEARCH INSTITUTE MATERIALS SAFETY TECHNOLOGY DEVELOPMENT DIVISION, , DAEJEON, 34057, REPUBLIC OF KOREA
[2] KOREA INSTITUTE OF MACHINERY AND MATERIALS, DEPARTMENT OF INDUSTRIAL LASER TECHNOLOGY, BUSAN, 46744, REPUBLIC OF KOREA
[3] KOREA ADVANCED INSTITUTE OF SCIENCE AND TECHNOLOGY, DEPARTMENT OF NUCLEAR AND QUANTUM ENGINEERING, DAEJEON, 34141, REPUBLIC OF KOREA

* Corresponding author: shkang77@kaeri.re.kr
† These authors contributed equally to this work.

Cr, and Y were charged to achieve Fe-14.6Cr-1.2Y (in wt.%) and placed in a ceramic crucible. Al_2O_3 and MgO ceramic crucibles were selected for comparison. The crucible was then induction heated to 1600°C under an argon atmosphere (3×10^{-2} torr), and the molten steel was poured into graphite ingot mold. The chemical composition of VIM processed steel was analyzed using inductively coupled plasma atomic emission spectrometer (ICP-AES, Thermo ICAP 6000). From now on, Y retained steel produced using an Al_2O_3 crucible is referred to as steel (Al_2O_3), while the steel produced using an MgO crucible is referred to as steel (MgO)

The cross section of samples were obtained by electrical discharge machining, followed by standard metallographic polishing. The microstructures were characterized by dual beam scanning electron microscope/focused ion beam (FIB; ThermoFisher Scios 2). The chemical composition of oxides and phases were analyzed by energy dispersive X-ray spectroscopy (EDS, Oxford Instruments; Ultimate Max). The phases present in steel (MgO) were further corroborated using X-ray diffraction (XRD, Rigaku SmartLab) and transmission electron microscopy (JEOL; JEM 2100F).

Thermodynamic Scheil simulation was performed using Thermo-Calc TCFE8 database.

3. Results and discussion

Fig. 1 shows the VIM processed steel fabricated using (a) Al_2O_3 crucible and (c) MgO crucible. The white particles labelled 1 and 2 in steel (Al_2O_3) were identified as Y-Al-O oxides, as summarized in TABLE 1. In contrast, white phases labelled 3 and 4 formed in steel (MgO) were confirmed as Fe-Y phase, as also summarized in TABLE 1. The Y content was measured to be 0.04 wt.% in steel (Al_2O_3), compared with 1.06 wt.% in steel (MgO) confirmed by ICP-AES. These results indicate that most of the initial Y content (1.2 wt.%) was oxidized to form Y-Al-O oxide in steel (Al_2O_3), whereas it remained predominantly as Fe-Y phases in steel (MgO).

TABLE 1

EDS results of Fig. 1

Position	Chemical composition (wt.%)				
	Fe	Cr	Y	Al	O
1	16.2	3.4	52.9	7.9	19.6
2	6.4	1.1	62.6	7.6	22.3
3	Bal.	9.6	13.7	—	—
4	Bal.	9.8	12.9	—	—

The Fe-Y phase observed in the steel (MgO), as shown in Fig. 1(d), was identified as Fe_5Y (PDF card No. 03-065-9148, space group P6/mmm) based on the XRD patterns presented in Fig. 2 XRD patterns. The matrix phase was detected as α-Fe (PDF card No. 01-080-3816, space group Im-3m). The weak diffraction peaks corresponding to Fe_5Y phase were further confirmed by selected area electron diffraction pattern (SADP), obtained from the scanning transmission electron microscope-high angle annular dark field (STEM-HAADF) image shown in Fig. 3(a). The zone axis of Fe_5Y SADP was indexed as $[1\bar{2}\bar{1}3]$ shown in Fig. 3(b). The SADP of Fig. 3(c) was confirmed to α-Fe zone axis $[\bar{1}11]$.

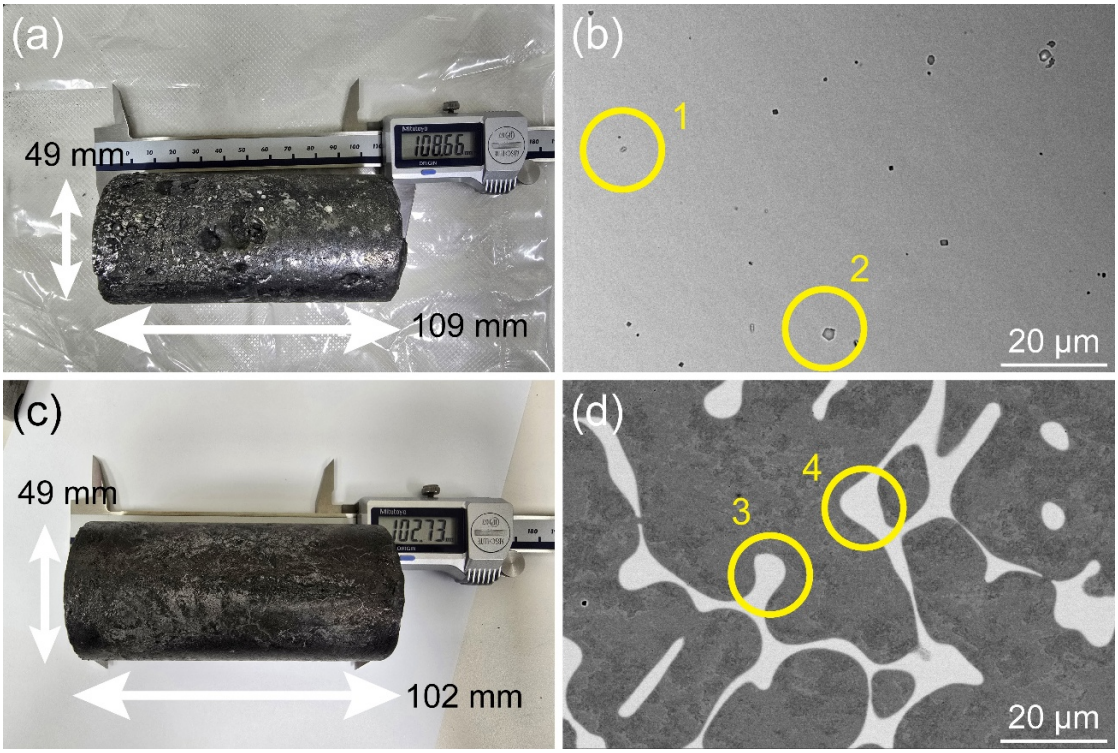

Fig. 1. Photography of (a) steel (Al_2O_3), and (c) steel (MgO). SEM-BSE image of (b) steel (Al_2O_3), (d) steel (MgO). The numbers and circle indicate the point EDS analysis and the results are summarized in TABLE 1

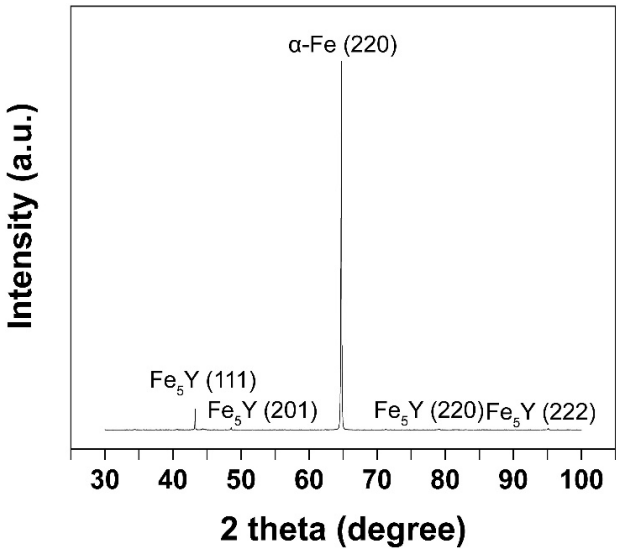

Fig. 2. XRD patterns of ODS steel (MgO)

In our study, a slight loss of Y was observed in the steel (MgO), with the Y content decreasing from the initial 1.2 wt.% to 1.06 wt.%, and the remaining Y existing predominantly as the Fe_5Y phase. According to the Fe-Y phase diagram, the maximum solubility of Y in Fe is approximately 1 wt.% [10]; therefore, the Y content in the steel (MgO) exceeds the solubility limit, leading to the formation of Fe-Y phases. During the solidification of steel (MgO, Fe-14.6Cr-1.06Y), the solidification trajectory stated in Fig. 3(d) vertical section is as follows: liquid(L) to L + α-Fe to L + α-Fe + $Fe_{17}Y_2$ and finally remaining liquid solidified to α-Fe + $Fe_{17}Y_2$. The equilibrium vertical section is just estimating the trajectory of solidification because the vacuum induction melting obeys non-equilibrium Scheil cooling [11] rather than equilibrium cooling. In Figs. 3(e) and 3(f), the Scheil simulation was conducted and during the cooling, the Y continuously enriched in remaing liquid and the Y content far exceeds the maximum solubility in Fe, 1 wt.% (weight fraction 0.01). As a result, the $Fe_{17}Y_2$ phase starts to evolve below 1240°C and ends at 1140°C.

Interestingly, the Fe_5Y phase in Figs. 2 and 3(b) was formed after VIM in the present study. Previous studies by Mihalkovič and Gruszka reported that metastable high temperature phase $Fe_{17}Y_2$ decomposes into Fe_5Y and α-Fe below 900°C [12,13]. As a result, in our study, during the solidification, $Fe_{17}Y_2$ initially evolved, as shown in Fig. 3(e), and subsequently decomposes into Fe_5Y and α-Fe, consistent with the experimental observations in Figs. 2 and 3(b).

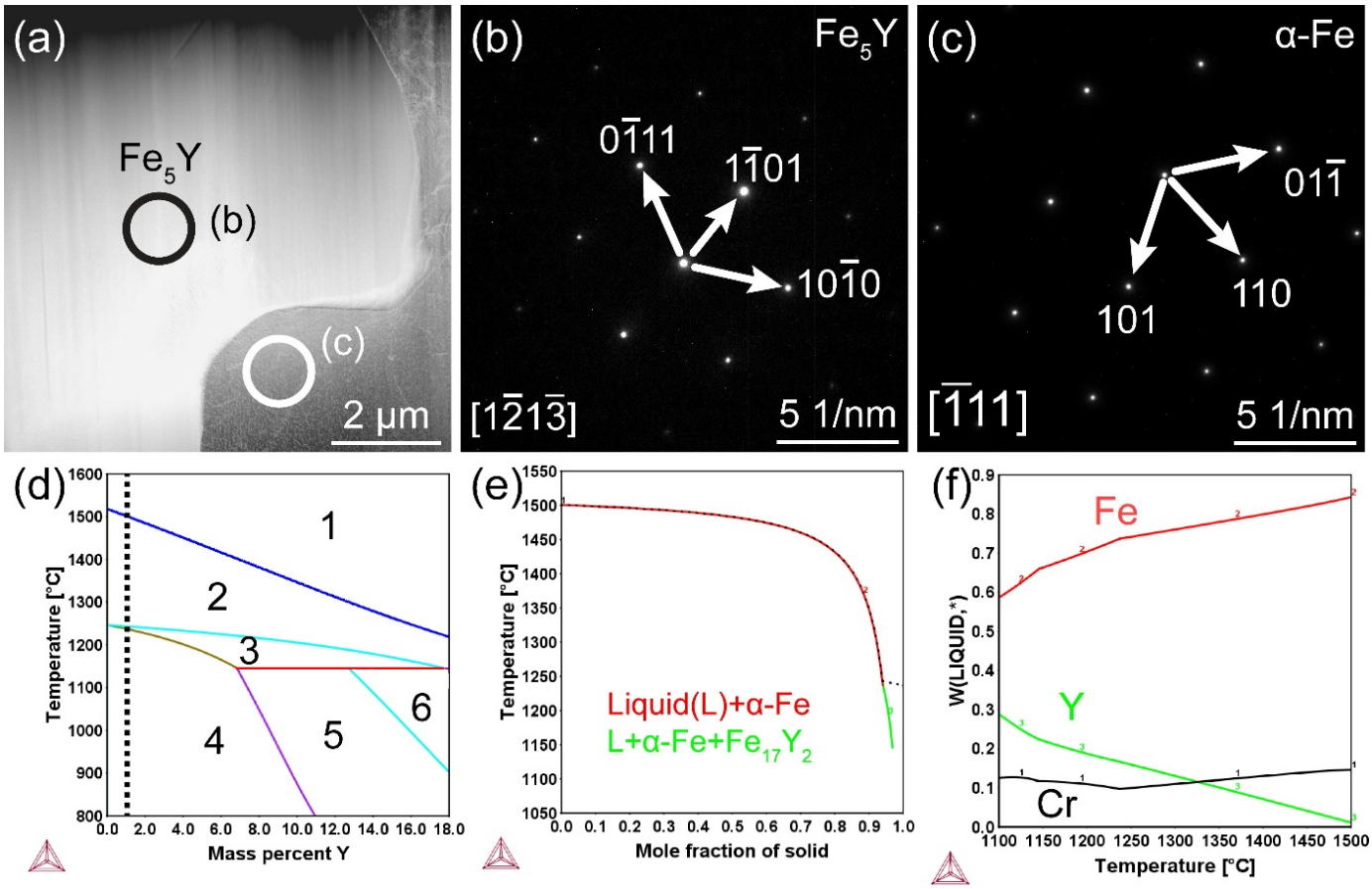

Fig. 3. (a) STEM-HAADF image in ferritic steel (MgO), SADP patterns of (b) Fe_5Y and (c) α-Fe matrix specified in (a). Vertical section of ternary system (d) Fe-14.6Cr-xY ($0 \leq x \leq 18$ wt.%). The black dashed line represents the composition of ferritic steel (MgO). The numbers indicate the region where the phases co-exist: 1. Liquid (L), 2. L + α-Fe, 3. L + α-Fe + $Fe_{17}Y_2$, 4. α-Fe + $Fe_{17}Y_2$, 5. α-Fe + $Fe_{17}Y_2$ + $Fe_{23}Y_6$, 6. α-Fe + $Fe_{23}Y_6$. (e) Scheil simulation of ferritic steel (MgO) and (f) compositional change of liquid phase depending on temperature. The W(liquid,*) indicates the weight fraction of elements in liquid phase

Compared with steel (Al_2O_3), only a slight low of Y was observed in steel (MgO). This behavior is attributed to the stronger and continuous reaction of Y with Al_2O_3 relative to MgO. The Y_2O_3-Al_2O_3 phase diagram indicates that Y_2O_3 is insoluble in Al_2O_3, leading to the formation of Y-Al-O oxides [14]. In contrast, Y_2O_3 is soluble to MgO [15]. Furthermore, when Y containing molten Fe comes into contact with MgO, a Y_2O_3 layer initially forms at the melt-crucible interface [16]. As a result, Y loss is minimized in ferritic steel fabricated using an MgO crucible, as the Y_2O_3 layer suppresses further interfacial reactions.

4. Conclusions

In this study, Y pre-alloyed ferritic steels were fabricated by vacuum induction melting using Al_2O_3 and MgO crucibles, revealing a strong dependence of Y retention on crucible material. In the Al_2O_3 crucible, most of the initial Y was consumed to form Y-Al-O oxides, resulting in a very low residual Y content of 0.04 wt.%. In contrast, the MgO crucible preserved Y effectively, yielding 1.06 wt.% Y that predominantly existed as Fe_5Y phases within an α-Fe matrix. Thermodynamic Scheil simulations indicated that $Fe_{17}Y_2$ initially forms during solidification. After that, $Fe_{17}Y_2$ subsequently decomposes into Fe_5Y and α-Fe, consistent with experimental observations. There results demonstrate that MgO crucibles are more suitable than Al_2O_3 crucibles for minimizing Y loss during VIM processing of Y pre-alloyed ferritic steels.

Acknowledgments

This work was supported by National Research Foundation of Korea (NRF) grants funded by the Ministry of Science and ICT (RS-2024-00402378), and Nano & Material Technology Development Program (RS-2024-00445448).

REFERENCES

[1] R.L. Klueh, Tensile and creep properties of an oxide dispersion-strengthened ferritic steel. J. Nucl. Mater. **307**, 773-777 (2002). DOI: https://doi.org/10.1016/S0022-3115(02)01046-2

[2] S. Kim, Effects of yttrium on the oxidation behavior of Fe13Cr6AlY alloys under 1200°C steam. J. Alloy. Compd. **960**, 170642 (2023). DOI: https://doi.org/10.1016/j.jallcom.2023.170642

[3] S.J. Zinkle, Development of next generation tempered and ODS reduced activation ferritic/martensitic steels for fusion energy applications. Nucl. Fusion. **57** (9), 092005 (2017). DOI: https://doi.org/10.1088/1741-4326/57/9/092005

[4] S. Ukai, Oxide dispersion-strengthened/ferrite-martensite steels as core materials for Generation IV nuclear reactors. In Structural materials for generation IV nuclear reactors, Woodhead Publishing (2017).

[5] G.R. Odette, Nano-oxide dispersion-strengthened steels. In Structural alloys for nuclear energy applications, Elsevier (2019).

[6] G.R. Odette, On the status and prospects for nanostructured ferritic alloys for nuclear fission and fusion application with emphasis on the underlying science. Scr. Mater. **143**, 142-148 (2018). DOI: https://doi.org/10.1016/j.scriptamat.2017.06.021

[7] D. Zhang, No ball milling needed: Alternative ODS steel manufacturing with gas atomization reaction synthesis (GARS) and friction-based processing. J. Nucl. Mater. **566**, 153768 (2022). DOI: https://doi.org/10.1016/j.jnucmat.2022.153768

[8] D. Pazos, ODS ferritic steels obtained from gas atomized powders through the STARS processing route: Reactive synthesis as an alternative to mechanical alloying. Nucl. Mater. Energy. **17**, 1-8 (2018). DOI: https://doi.org/10.1016/j.nme.2018.06.014

[9] M. Dejong, Variations in GARS powder microstructure as a function of powder chemistry and particle size. Powder Technol. **455**, 120734 (2025). DOI: https://doi.org/10.1016/j.powtec.2025.120734

[10] B.W. Zhang, The Fe-Y (iron-yttrium) system. J. Ph. Equilibria. **13** (3), 304-308 (1992). DOI: https://doi.org/10.1007/bf02667560

[11] Y. N. Wang, The effect of cooling conditions on the evolution of non-metallic inclusions in high manganese TWIP steels. Metall. Mater. Trans. B. **47** (2016), 1378-1389. DOI: https://doi.org/10.1007/s11663-015-0568-7

[12] M. Mihalkovič, Ab initio calculations of cohesive energies of Fe-based glass-forming alloys. Phys. Rev. B Condens. Mater. **70** (14), 144107 (2004). DOI: https://doi.org/10.1103/PhysRevB.70.144107

[13] K. Gruszka, Analysis of the structure (XRD) and microstructure (TEM, SEM, AFM) of bulk amorphous and nanocrystalline alloys based on FeCoB. Int. J. Mater. Res. **106**, 689-696 (2015). DOI: https://doi.org/10.3139/146.111226

[14] O. Fabrichnaya, The assessment of thermodynamic parameters in the Al2O3-Y2O3 system and phase relations in the Y-Al-O system. Scand. J. Metall. **30** (3), 175-183 (2001). DOI: https://doi.org/10.1034/j.1600-0692.2001.300308.x

[15] Y. Du, Thermodynamic assessment of the $YO_{1.5}$-MgO system. J. Alloys. Compd. **176** (1), L1-L4 (1991).

[16] J. Kang, Steel-refractory reactions in lanthanum-, cerium-, and yttrium-added steels. J. Iron Steel Res. Int. **31** (6), 1473-1485 (2024). DOI: https://doi.org/10.1007/s42243-023-01163-5